

## Article

# Enhancement of Dye Separation Performance of Eco-Friendly Cellulose Acetate-Based Membranes

Omneya A. Koriem <sup>1,\*</sup>, Alaa Mostafa Kamel <sup>1</sup>, Waleed Shaaban <sup>2</sup> and Marwa F. Elkady <sup>1,3,\*</sup>

<sup>1</sup> Chemical and Petrochemical Engineering Department, Egypt-Japan University of Science and Technology, New Borg El-Arab City, Alexandria 21934, Egypt

<sup>2</sup> Mechanical Engineering Department, Mansoura University, El-Mansoura 35516, Egypt

<sup>3</sup> Fabrication Technology Department, Advanced Technology and New Materials Research Institute (ATNMRI), City of Scientific Research and Technological Applications, New Borg El-Arab City, Alexandria 21934, Egypt

\* Correspondence: omneya.koriem@ejust.edu.eg (O.A.K.); marwa.elkady@ejust.edu.eg (M.F.E.)

**Abstract:** Many reasons have caused a worldwide water stress problem. Thus, the recycling of wastewater streams has been extensively studied. In this work, eco-friendly mixed matrix membranes (MMMs) were fabricated, characterized, and tested for the removal of two separate dyes from simulated waste streams. The environmentally friendly nano activated carbon (NAC) was extracted from water hyacinth to be impregnated as a membrane nano-filler to enhance the neat membrane performance. The extracted NAC was further studied and characterized. Cellulose acetate (CA)-based membranes were obtained by phase inversion and electrospinning mechanisms. All four synthesized blank and MMMs were characterized via scanning electron microscope (SEM) and contact angle to study their structure and hydrophilic nature, respectively. However, the membrane with optimum performance was further characterized using Fourier transfer infrared (FTIR) and X-ray diffraction (XRD). The four prepared cast and electro-spun, blank, and mixed matrix CA-based membranes showed an acceptable performance in the removal and selectivity of methylene blue (MB) dye over Congo red (CR) dye with a removal percentage ranging from 31 to 70% depending on the membrane used. It was found that the CA/NAC hybrid nanofiber membrane possessed the highest removal efficiency for MB, where the dye concentration declined from 10 to 2.92 mg/L. In contrast, the cast blank CA membrane showed the least removal percentage among the synthesized membranes with only 30% removal. As a result, this paper suggests the use of the CA/NAC hybrid membrane as an alternative and cost-effective solution for MB dye removal.

**Keywords:** adsorption; membrane; adsorptive membrane; activated carbon; dye removal; hybrid membrane



**Citation:** Koriem, O.A.; Kamel, A.M.; Shaaban, W.; Elkady, M.F.

Enhancement of Dye Separation Performance of Eco-Friendly Cellulose Acetate-Based Membranes. *Sustainability* **2022**, *14*, 14665. <https://doi.org/10.3390/su142214665>

Academic Editor: Andrea G. Capodaglio

Received: 14 September 2022

Accepted: 1 November 2022

Published: 8 November 2022

**Publisher's Note:** MDPI stays neutral with regard to jurisdictional claims in published maps and institutional affiliations.



**Copyright:** © 2022 by the authors. Licensee MDPI, Basel, Switzerland. This article is an open access article distributed under the terms and conditions of the Creative Commons Attribution (CC BY) license (<https://creativecommons.org/licenses/by/4.0/>).

## 1. Introduction

Due to globalization and the developed human lifestyle, dyes are widely used in various industrial fields. They are extensively used not only in the textile and paper industries, but also in food, pharmaceuticals, cosmetics, and many other vital industries [1]. In aqueous solutions, dyes are classified into two main categories: anionic and cationic [2]. It is estimated that around 10% of the textile industry's dyes are lost directly into water streams [3]. Even in low concentrations, most synthetic dyes have a harmful impact on flora and fauna, humans, and the environment. They are generally characterized by their toxicity, carcinogenic effects, and high color visibility [4–6]. Furthermore, they prevent the penetration of oxygen and sunlight into water systems. Consequently, they affect the photosynthetic ability of the flora, causing harm to aquatic life [7,8]. In addition, they are hardly removed from water bodies due to their high stability and water solubility [9–11]. As a result of the current water depletion situation, the available water sources need to be protected [12]. Accordingly, discharging industrial untreated waste streams containing dye contamination

is considered one of the main environmental problems that require immediate intervention. As a result, many researchers are eager to discover cost-effective and eco-friendly techniques to discard dyes and other pollutants from waterways [13–16]. Up to this point, numerous methods have been utilized in dye removal from waste streams. They can be categorized into physical, chemical, biological, or hybrid methods [17]. Those methods, including but not limited to, coagulation [18], adsorption [19], photolysis [20], electrochemical [21], biological treatment [22], membrane processes [23], and their hybrids [24–26] have all been investigated. Amongst them, adsorption is used for its efficiency, easy processing, and cheap cost [27], while membranes are used for their low required energy, low required space, reduced chemical consumption, and relatively low cost of operation [6]. However, they still have some limitations and drawbacks. Thus, the hybrid adsorptive membranes concept was investigated by incorporating adsorptive nanoparticles (NPs) into the synthesized membranes, resulting in a membrane that has the ability to possess the function of both systems [28–30].

For the process to be as effective as possible, the polymeric membrane material and the suitable incorporated adsorbent should be selected carefully. According to the literature, chitosan [31], alginate [32], and cellulose acetate [33] have been previously investigated for dye removal for their eco-friendly characteristics and removal efficiency. Amongst them, cellulose acetate (CA) has been extensively used because it is a biodegradable, low-cost, easily tailored, and available biopolymer [33,34]. Moreover, it is well known for its chemical and thermal stability [35]. Despite that, its inferior adsorption efficiency lessens its application for dye removal [36]. Therefore, impregnating adsorptive particles within CA may enhance the neat membrane adsorptive capacity [37]. The mechanism of adsorptive membranes depends on two steps: rejection and adsorption. In the rejection step, the particles with sizes larger than the pore size of the membrane are rejected by the membrane's surface, or what is called the membrane's active layer. In the next step, adsorption takes place, where small particles react or attach to the impregnated adsorbent, which in turn increases the overall removal efficiency of the membrane [38]. Previously, various adsorbents were tested for dye removal, namely zeolites, clay, limestone, lignite, and graphene oxide [39,40]. Among the most commonly used adsorbents, activated carbon (AC) is recognized as a perfect adsorbent for dye removal [41]. AC has an undoubtable dye removal performance, and it has previously proven to be a competitive adsorbent. AC is well known for its high adsorption capacity, large porous structure, high available active sites, and large surface area [42,43]. Additionally, nano activated carbon (NAC) is characterized by a much higher surface area and in return better adsorption capacity over AC [44]. Nevertheless, it has some limitations due to its high cost and non-renewable source. Thus, many studies have been conducted in order to provide an alternative low-cost adsorbent [34,45]. Agricultural wastes provide a competitive raw material for obtaining cheap, efficient, and renewable ACs [46]. Water hyacinth is an unwanted waste that can cause severe damage to aquatic life [47]. The control of water hyacinth is an effort, time, and money-consuming problem. Consequently, turning this irritating plant into an effective bio-sorbent could be more valuable [48,49].

To the best of the authors' knowledge, there is no other study that has investigated the impregnation of NAC fabricated from agricultural waste with blank cast and electro-spun CA-based membranes for dye decontamination from polluted water. Accordingly, in the current study, eco-friendly CA-based membranes were synthesized via phase inversion and electrospinning techniques. Additionally, nano activated carbon (NAC) was fabricated from Egyptian water hyacinths. The effect of impregnating the synthesized NAC bio-sorbent into the cast and the nanofibrous membranes was investigated. Methylene blue (MB) and Congo red (CR) were selected as cationic and anionic dyes, respectively. The selectivity of the fabricated, cast and electro-spun, neat CA and hybrid CA/NAC membranes towards MB and CR was studied.

## 2. Materials and Methods

### 2.1. Materials

All chemicals included in this study were used as purchased without any further modification. Cellulose acetate (CA) polymer with a molecular weight of 30,000 was supplied by Lobachemie, acetone (ACS > 99.5%) and dimethylformamide (DMF > 99.9%) were purchased from Fisher, sodium hydroxide (NaOH), methylene blue (MB) dye, and Congo red (CR) dye, and distilled water were bought from Sigma Aldrich. Additionally, activated carbon was prepared from Egyptian water hyacinth, which was collected from Itay El-Baroud Drainage, Al-Buhayrah governorate, Egypt.

### 2.2. Synthesis of Nano Activated Carbon (NAC)

Water hyacinth roots were used as the precursor for the preparation of dye removal bio-sorbent material [50]. To remove dust or any trapped particles, the collected raw precursor was rinsed extensively with distilled water. The washed water hyacinth was then dried in an electrical oven before being crushed into a fine powder. Then, for alkaline chemical treatment, 1 g of the obtained powder was further suspended in 100 mL of 2 M NaOH for 1 h under stirring at 60 °C. The chemically treated materials were then filtered and washed several times to get rid of any basic or acidic residuals. The treated washed materials were finally dried overnight at 70 °C, followed by a carbonization process in an Across muffle furnace for 1 h at 600 °C.

### 2.3. Synthesis of Neat and Composite CA-Based Dope Solutions

For the neat CA membrane, a suitable amount of CA polymeric powder was dissolved in a binary solvent mixture of acetone and DMF with a ratio of 2:1, respectively, to prepare a 15 wt% of neat CA dope solution. On the other hand, 5 wt% of the nano-filler (NAC) was sonicated firstly with the same binary solvent mixture for 1 h before the CA powder was added and stirred with it to obtain the composite CA/NAC dope solution. The previous solutions were then used to fabricate the neat and composite CA-based membranes via phase inversion and electrospinning techniques.

#### 2.3.1. Synthesis of Cast Neat and Composite CA-Based Membranes

The membrane phase inversion method has been used for many years for the fabrication of flat sheet polymeric membranes [51–53]. The previously prepared blank CA and composite CA/NAC dope solutions were cast on a clean glass plate at room temperature. A doctor knife blade with a micrometer fixed at 0.25 mm was used to prepare the membranes with the required thickness. The cast films were left to evaporate in the air for 60 s before being immersed at (0–4 °C) in a distilled water bath. The obtained flat sheet membrane was then rinsed to get rid of any residual solvent. As a final treatment step, the membrane was then annealed at 80 °C for 10 min in another distilled water bath. The fabricated membranes were preserved in distilled water for at least 24 h for further use and characterization.

#### 2.3.2. Synthesis of Electro-Spun Nanofibrous Neat and Composite CA-Based Membranes

Thanks to the electrospinning technique, the fabrication of nanofibrous membranes is possible. Due to the outstanding properties of higher surface area as well as higher membrane porosity [54,55], the technique was investigated. The pristine CA and hybrid CA/NAC polymeric solutions were spun with the help of (NanoNC) electro-spinning equipment under different conditions of feed pumping flow rate, applied voltage, and tip-to-collector distance. The optimum nanofibrous membrane was obtained at operating conditions of 0.7 mL/h, 19 kV, and 15 cm, respectively. The fabricated nanofiber membranes were then left to dry in a drying oven overnight for further use and characterization.

### 2.4. Characterization of the Extracted NAC and Fabricated CA-Based Membranes

Various techniques were involved in characterizing the synthesized electro-spun and cast CA-based membranes as well as the extracted NAC. Fourier transform infrared

spectroscopy (FTIR) (Bruker Vertex 70) was used to observe and confirm the presence of the functional groups of the used materials. A Shimadzu XRD-6100 X-ray diffraction (XRD) device was used to study the crystalline nature of the fabricated membranes. The spectra were recorded from 3500 to 500  $\text{cm}^{-1}$ .

The morphology of the membranes and the extracted NAC was investigated using a scanning electron microscope (SEM) device (JOEL JSM-6010 LV). The hydrophilic/hydrophobic nature of the membranes was measured using a contact angle system (DSA 100, KRÜSS). For more accurate results, five random locations on each membrane surface were selected to measure the contact angle.

### 2.5. Performance Testing of the Synthesized Electro-Spun and Cast CA-Based Membranes

In this study, the performance of the fabricated neat and hybrid membranes in the removal of cationic (MB) and anionic (CR) dyes was investigated. All decolorization experiments were repeated 4 times and the average measurements were recorded for more accuracy. Accordingly, as shown in Figure 1, each membrane's efficiency was evaluated using an Amicon cell setup with an active filtration area of around 480  $\text{mm}^2$ . Each membrane was divided into circular shapes similar to the active area of the cell. Two stock solutions of MB and CR, 10 ppm each, were prepared to simulate the industrial dye-containing waste streams. At room temperature, the cell was then filled with the dye solution and connected to a syringe pump to apply a small pressure that allowed the water to flow through the membrane. The filtrate was recirculated until equilibrium was reached. A sample of the filtrate of each cycle was taken and the dye concentration was measured using a spectrophotometer device.

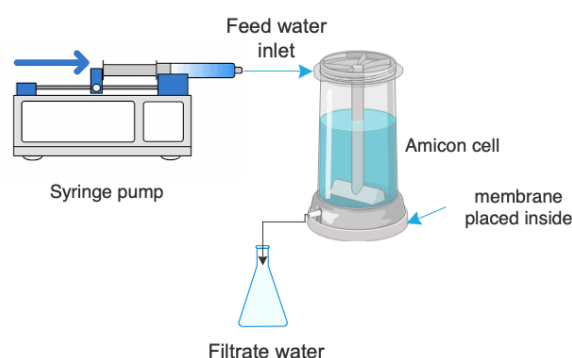


**Figure 1.** Amicon cell filtration setup.

The rejection factor (R) was calculated from Equation (1)

$$\%R = \left(1 - \frac{C_P}{C_R}\right) \quad (1)$$

where  $C_P$  and  $C_R$  are the dye concentrations of the filtrate and the feed solution (mg/L), respectively.

## 3. Results and Discussion

### 3.1. Characterization of Nano Activated Carbon (NAC)

As the functional groups of the obtained NAC have an impact on the adsorption efficiency [56], FTIR was used to recognize those functional groups. As can be seen in Figure 2a, the peak at 3401  $\text{cm}^{-1}$  refers to the O-H functional group, which gives an indication of the bonded hydroxide in the prepared NAC. The band found at 1635  $\text{cm}^{-1}$  could be due to C=C or C=O stretching [57]. The broad band found at 1157  $\text{cm}^{-1}$  suggests the surface group of C-O stretching [58]. The absorption band at 616  $\text{cm}^{-1}$  might refer to the C-H stretching or C=O bonding [59].

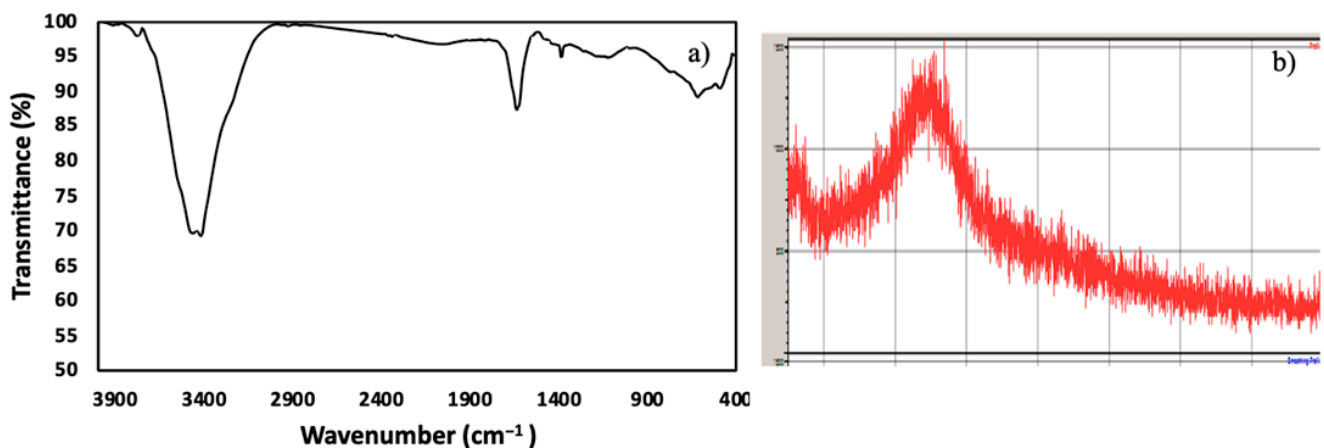


Figure 2. (a) FTIR spectrum (b) XRD pattern of the fabricated nano activated carbon NAC.

The XRD pattern was investigated in order to study the crystalline nature of the prepared NAC. As illustrated in Figure 2b, the obtained NAC has a semi-crystalline structure. In addition, the appearance of a broad peak in the range of  $22^\circ$  to  $24^\circ$  indicates the existence of carbon. On the other hand, the absence of other characteristic peaks gives an indication of the absence of any other contaminants [60].

The morphology of the prepared NAC was investigated by SEM images as presented in Figure 3a. SEM micrographs confirmed that a uniform nanosized material was obtained and the average diameter of the fabricated particles was estimated at 58 nm.

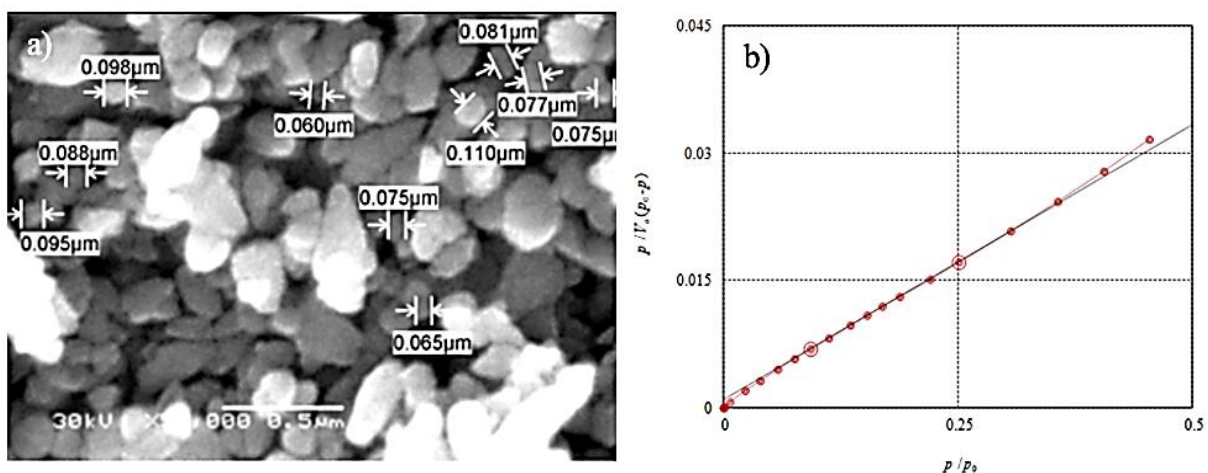


Figure 3. (a) SEM image (b) BET of the fabricated nano activated carbon (NAC).

The BET surface area of the fabricated NAC was measured to evaluate the material pore size, pore volume, and surface area. As shown in Figure 3b, N<sub>2</sub> adsorption/desorption isotherm of the synthesized bio-sorbent was investigated. The NAC surface area was found to be  $66.2 \text{ m}^2/\text{g}$ . On the other hand, the total pore volume was measured as  $0.25 \text{ cm}^3/\text{g}$ , while its average pore size was recorded as 15.2 nm.

### 3.2. Characterization of Cast and Electro-Spun Neat and Composite CA-Based Membranes

As illustrated in Figure 4, the surface and cross-sectional structure of the cast neat CA and composite CA/NAC membranes was investigated via SEM images. Compared to the clear neat surface of CA, Figure 4a, the impregnated NAC clearly appears as white particles on the surface of the membrane in Figure 4b. This could give an indication of the successful dispersion of the NAC particles within the dope solution. In addition, from the cross-sectional images, it can be seen that the addition of NAC particles transformed

the structure of the blank CA membrane, Figure 4c, into a more porous structure. A few longitudinal pores of the composite CA/NAC membrane are demonstrated in Figure 4d.

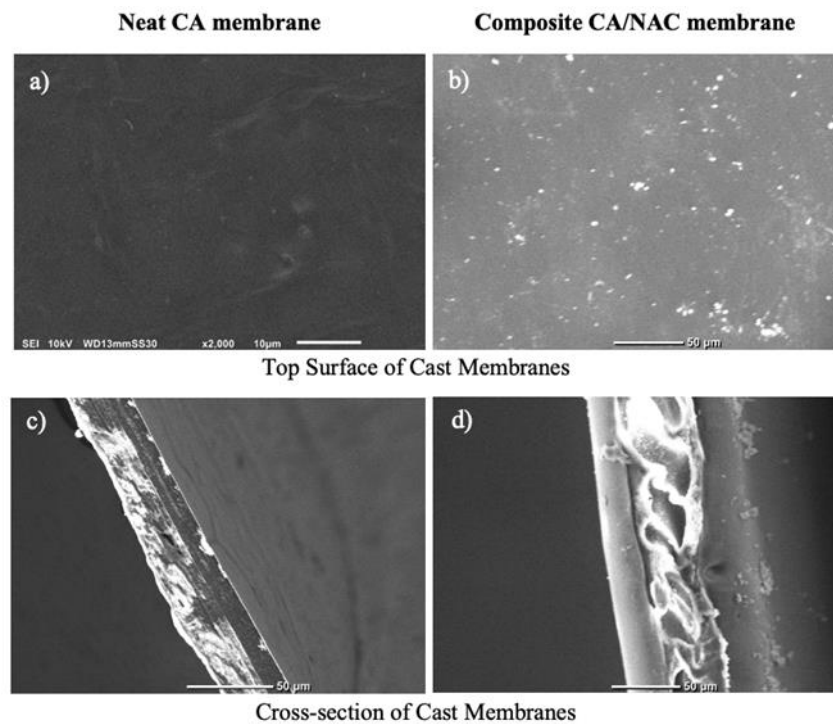


**Figure 4.** SEM images of cast membranes of “(a,c)” CA and “(b,d)” CA/NAC nanofiber membranes.

The optimum electro-spinning operating conditions were selected depending on the fiber shapes and diameters. The optimum conditions were used to fabricate a full matrix of CA and CA/NAC. The difference in the morphological structure between the synthesized blank and composite CA membranes can be seen in Figure 5. SEM images illustrate that both CA and CA/NAC membranes have uniform, straight, and bead-less fibers. In Figure 5a, the blank CA membrane nanofibers are shown as a uniform clear network. However, in Figure 5b, the loaded NAC can be seen as white dispersed particles and show good distribution with no agglomerations.

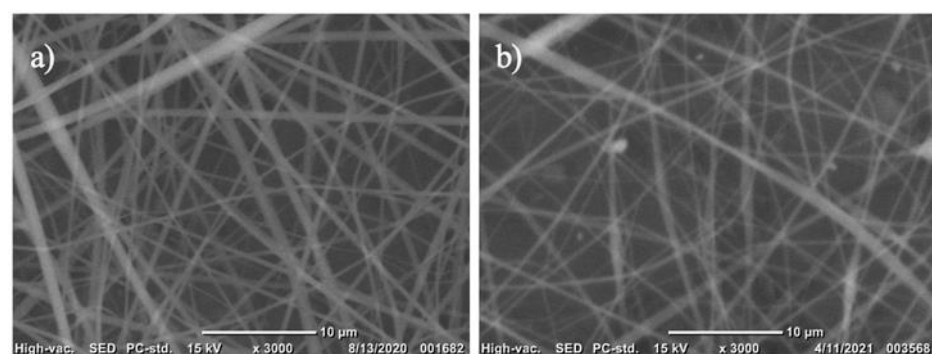


**Figure 5.** SEM images of “(a)” CA and “(b)” CA/NAC nanofiber membranes.

The surface wettability of the four fabricated cast and electro-spun membranes was investigated in order to study the effect of membrane surface morphology on the contact angle of each membrane. The hydrophilicity of the surface of the membrane affects the filtration flux [42]. The contact angle was expected to be less than  $90^\circ$  to be hydrophilic. Additionally, it was expected from the literature that the nanofibrous mat would be more hydrophilic than the cast one [61]. As displayed in Figure 6, all four membranes were found

to be hydrophilic to different degrees. The contact angle of the blank cast and nanofiber membranes decreased after the addition of NAC particles. The contact angle of the blank CA cast membrane decreased from  $63.5^\circ$  to  $58.6^\circ$ , while it lowered from  $60.5^\circ$  for the neat CA nanofibrous membrane to become  $58^\circ$  for the composite CA/NAC nanofibrous membrane. This means that the addition of NAC has enhanced the membrane's hydrophilicity, which is an important and crucial parameter in water filtration.

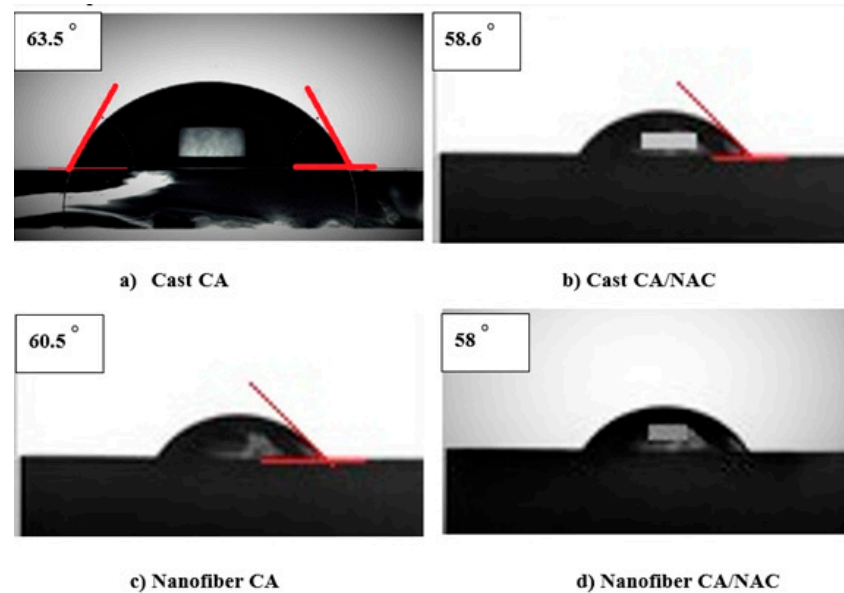


**Figure 6.** Contact angle of cast and electro-spun neat and composite CA-based membranes.

For nanofibrous blank CA and mixed matrix CA/NAC, FTIR spectra were further used to study the functional groups of both membranes. As demonstrated in Figure 6a, a wide band at  $3395\text{ cm}^{-1}$  represents the presence of hydroxyl ( $-\text{OH}$ ) stretching [62]. This band was shifted to  $3474\text{ cm}^{-1}$  and its intensity decreased with the addition of NAC, as seen in Figure 7b. The carbonyl ( $\text{C}=\text{O}$ ) group was observed at  $1731\text{ cm}^{-1}$ . The adsorption peak at  $1428\text{ cm}^{-1}$  refers to the ( $\text{CH}_2$ ) deformation vibration. The characteristic ( $\text{C}-\text{O}-\text{C}$ ) group can be seen at  $1225\text{ cm}^{-1}$ . However, as represented in Figure 7b, this adsorption peak was shifted to become  $1218\text{ cm}^{-1}$ . The stretching vibration of ( $\text{C}-\text{OH}$ ) in the blank CA membrane was illustrated at  $1029\text{ cm}^{-1}$  [63].

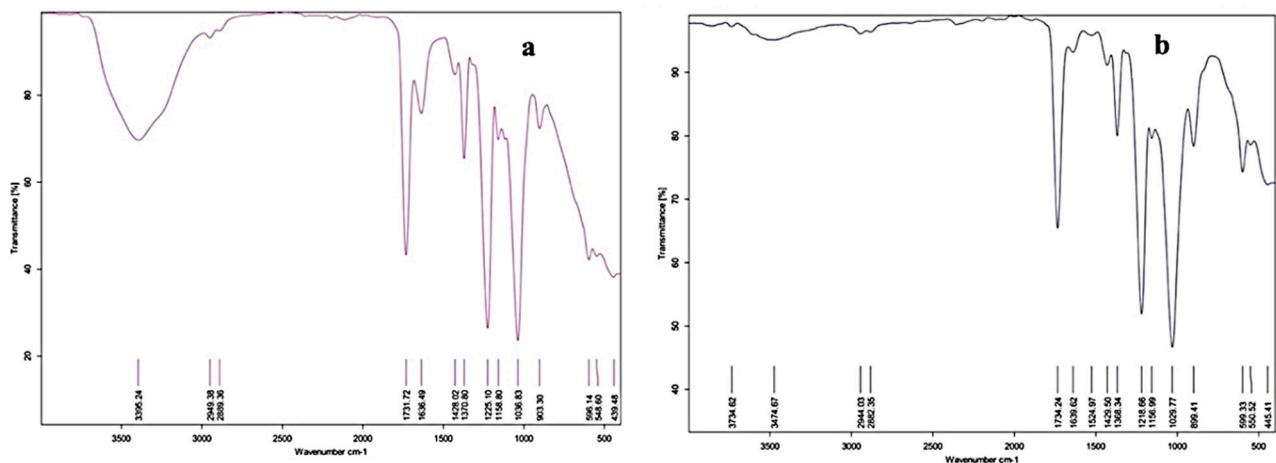


**Figure 7.** FTIR spectrum of “(a)” blank CA and “(b)” composite CA/NAC nanofibrous membranes.

As displayed in Figure 8, XRD was further used to give an indication of the successful impregnation of NAC. Figure 8a depicts the CA characteristic peaks at 10 and 20° [64]. Nonetheless, the intensity of the peak at 20° increased significantly.

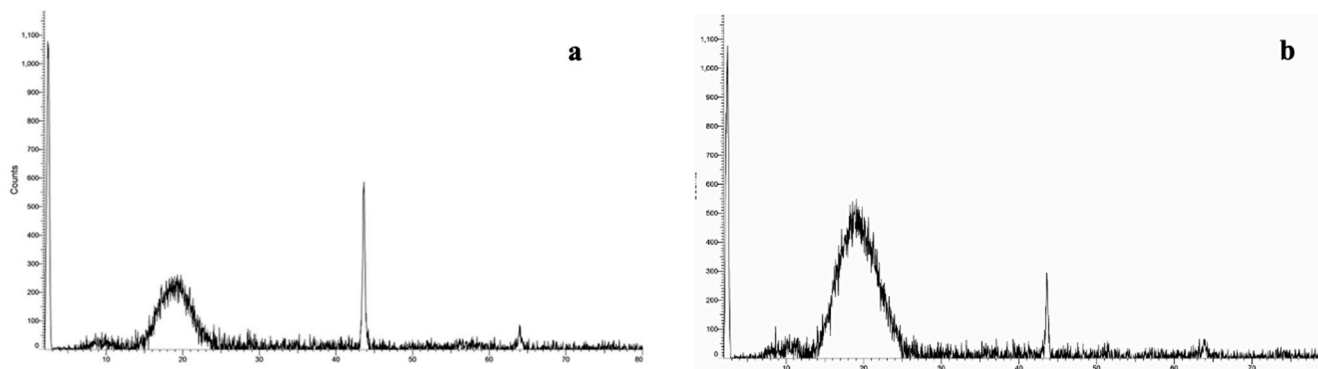


Figure 8. XRD pattern of (a) blank CA and (b) composite CA/NAC nanofibrous membranes.

This might be explained by the presence of carbon atoms and in return the impregnation of NAC particles.

### 3.3. Filtration Performance of Cast and Electro-Spun Neat and Composite CA-Based Membranes

The filtration performance of both blank and composite CA-based membranes for the removal of cationic MB and anionic CR was investigated using the previously mentioned Amicon cell setup. Generally, the four membranes showed a better affinity towards MB removal than CR. As illustrated in Figures 9 and 10, all the membranes had a noticeable effect on MB final concentration, while they had a negligible effect on CR final concentration.

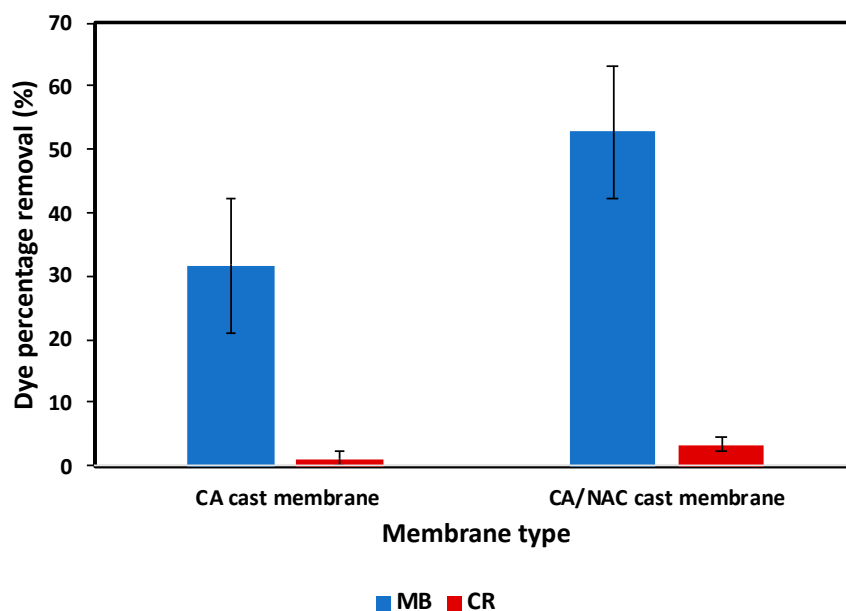
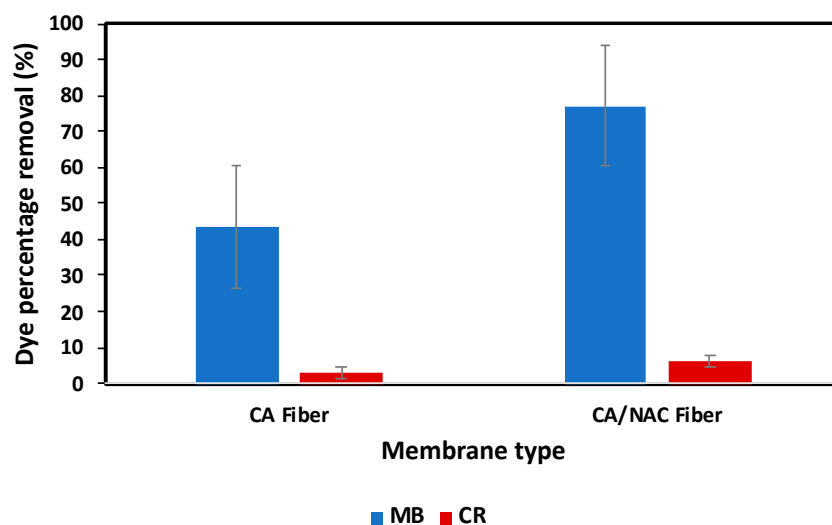


Figure 9. Performance of blank and composite cast membranes on the removal of MB and CR.





**Figure 10.** Performance of blank and composite nanofibrous membranes on the removal of MB and CR.

As clarified in Figure 9, the equilibrium concentration of the MB on the blank CA cast membrane was reached at 6.84 ppm with a removal percentage of 31.6%. However, the equilibrium concentration of CR on the same membrane was reached at 9.89 ppm with only 1.1% removal.

From Figure 9, it was noticed that the addition of NAC had a positive effect on the performance of the blank membrane. As illustrated, the equilibrium concentration of MB was reduced to be reached at 4.73 ppm, with around 53% removal for the cast CA/NAC composite membrane. However, this removal percentage is considered higher than that of the early reported cast CA/MWCNTs membrane. It was found that for 5 mg/L MB concentration, the recorded removal was less than 30% [65]. Unfortunately, regarding CR, the equilibrium concentration was affected slightly by the addition of NAC and was reached at 9.67 ppm to achieve a low removal percentage of only 3.3%.

On the other hand, the performances of the blank and impregnated CA-based nanofiber membranes are demonstrated in Figure 10. The fibrous membranes were also selective for MB over CR. The equilibrium concentration of MB over the blank CA fibrous membrane was found to be 5.67 ppm and after the addition of NAC, it became even lower until it reached almost 2.92 ppm. In other words, MB was removed using blank and impregnated fiber membranes by 43% and 70%, respectively.

On the contrary, CR reached the equilibrium concentration at 9.73 ppm using the blank CA fiber membrane and 9.41 ppm using the impregnated CA/NAC fiber membrane. The removal of CR using blank CA and impregnated CA/NAC fiber membranes was recorded at very small amounts of 2.7% and 5.9%, sequentially.

The presence of both the acetyl ( $\text{CH}_3\text{CO}^-$ ) and the hydroxyl ( $\text{OH}^-$ ) groups led to the negatively charged surface of the CA-based membranes. Thus, the selective behavior and better performance of CA-based membranes towards MB over CR could be due to the electrostatic interaction that takes place between MB molecules (positively charged) and the membrane surface (negatively charged) [30].

Regarding MB removal, Figure 11 compares the performance of the four membranes. Overall, the performance of fibers was better than that of cast membranes. At equilibrium, CA fiber removed 43.3% of methylene blue, while the blank cast membrane removed only 31%. The CA/NAC fiber presented the best behavior in removing the MB dye as it removed more than 70% of the dye. The removal of MB dye on the CA/NAC fiber at a neutral pH value was higher than that of the previously investigated CA/GO/TiO<sub>2</sub>-NH<sub>2</sub> composite membrane. The literature reported that MB removal efficiency was about 60% at pH = 7 [66]. To conclude, the addition of NAC improved the performance of the blank CA membranes. This might be due to the existence of NAC resulting in an increase in the available active adsorbent sites in the fabricated adsorptive membranes. Those active sites

may have captured more MB molecules within its porous structure, and this led to the enhancement of the blank CA membrane's performance [30].

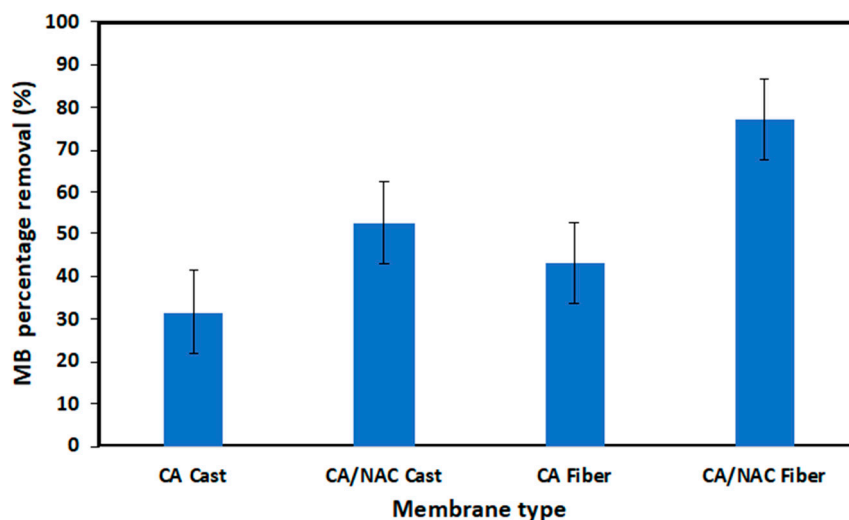


**Figure 11.** Comparison between the performance of the fabricated cast and nanofibrous CA-based membranes on the removal of MB dye.

#### 4. Conclusions

The current study used water hyacinth biomass as a raw material for the extraction of nano activated carbon to be used as a filler to enhance the performance of the blank CA membrane for water treatment. Through this study, the problem of water hyacinth spreading as a biomass waste could be solved. In addition, a more useful and cheaper bio-sorbent filler can be synthesized from this waste by a simple and facile technique. In return, this will help in solving an irritating water pollution problem. The characteristics of the synthesized NAC and the four fabricated membranes were studied by SEM, FTIR, and XRD. All the used techniques have allowed the successful impregnation of NAC into CA membranes. SEM images displayed the surface characteristics of NAC as well as all the fabricated membranes. FTIR and XRD were used to investigate and confirm the differences between the neat and composite CA-based membranes. In addition, the contact angle was used to explore the membrane hydrophilicity. The results showed the hydrophilic nature of all the fabricated membranes. Moreover, it proved that the nanofibrous mat had a better hydrophilic nature than the cast one. The performance of the four membranes was evaluated using an Amicon cell setup. It was found that all the membranes had a better removal selectivity towards MB dye than CR. Furthermore, the addition of NAC enhanced the blank CA membrane dye removal efficiency. Among the four tested membranes, the composite cast and electro-spun CA/NAC recorded the best performances of 52.7 and 70%, respectively. However, the performance of the neat cast and electro-spun CA membrane achieved only 30 and 43.3%. In conclusion, the nanofibrous membrane showed a better performance than the cast membranes. Moreover, the impregnation of NAC had a positive effect on the membrane dye removal efficiency.

**Author Contributions:** Writing—original draft, O.A.K., A.M.K. and M.F.E.; validation, O.A.K., A.M.K., W.S. and M.F.E.; investigation, O.A.K. and A.M.K.; formal analysis, M.F.E. and W.S.; writing—review and editing, O.A.K., A.M.K., W.S. and M.F.E.; methodology, M.F.E.; supervision, M.F.E. and W.S. All authors have read and agreed to the published version of the manuscript.

**Funding:** This research received no external funding.

**Institutional Review Board Statement:** Not applicable.

**Informed Consent Statement:** Not applicable.

**Data Availability Statement:** All data are provided.

**Conflicts of Interest:** The authors declare no conflict of interest.

## References

1. Li, Z.; Hanafy, H.; Zhang, L.; Sellaoui, L.; Netto, M.S.; Oliveira, M.L.S.; Seliem, M.K.; Dotto, G.L.; Bonilla-Petriciolet, A.; Li, Q. Adsorption of Congo red and methylene blue dyes on an ashitaba waste and a walnut shell-based activated carbon from aqueous solutions: Experiments, characterization and physical interpretations. *Chem. Eng. J.* **2020**, *388*, 124263. [[CrossRef](#)]
2. Xiao, J.; Lv, W.; Xie, Z.; Tan, Y.; Song, Y.; Zheng, Q. Environmentally friendly reduced graphene oxide as a broad-spectrum adsorbent for anionic and cationic dyes: Via  $\pi$ - $\pi$  Interactions. *J. Mater. Chem. A* **2016**, *4*, 12126–12135. [[CrossRef](#)]
3. Adesina, A.O.; Elvis, O.A.; Mohallem, N.D.S.; Olusegun, S.J. Adsorption of Methylene blue and Congo red from aqueous solution using synthesized alumina–zirconia composite. *Environ. Technol.* **2021**, *42*, 1061–1070. [[CrossRef](#)]
4. Ardila-Leal, L.D.; Poutou-Piñales, R.A.; Pedroza-Rodríguez, A.M.; Quevedo-Hidalgo, B.E. A brief history of colour, the environmental impact of synthetic dyes and removal by using laccases. *Molecules* **2021**, *26*, 3813. [[CrossRef](#)]
5. Ganapuram, B.R.; Alle, M.; Dadigala, R.; Dasari, A.; Maragoni, V.; Guttena, V. Catalytic reduction of methylene blue and Congo red dyes using green synthesized gold nanoparticles capped by *Salmaalina malabarica* gum. *Int. Nano Lett.* **2015**, *5*, 215–222. [[CrossRef](#)]
6. Moradihamedani, P. Recent advances in dye removal from wastewater by membrane technology: A review. *Polym. Bull.* **2022**, *79*, 2603–2631. [[CrossRef](#)]
7. Sharma, J.; Sharma, S.; Soni, V. Classification and impact of synthetic textile dyes on Aquatic Flora: A review. *Reg. Stud. Mar. Sci.* **2021**, *45*, 101802. [[CrossRef](#)]
8. Chowdhury, S.; Pan, S.; Balasubramanian, R.; Das, P. Date Palm Based Activated Carbon for the Efficient Removal of Organic Dyes from Aqueous Environment. In *Sustainable Agriculture Reviews 34: Date Palm for Food, Medicine and the Environment*; Naushad, M., Lichtfouse, E., Eds.; Springer International Publishing: Cham, Switzerland, 2019; pp. 247–263. [[CrossRef](#)]
9. Lellis, B.; Fávoro-Polonio, C.Z.; Pamphile, J.A.; Polonio, J.C. Effects of textile dyes on health and the environment and bioremediation potential of living organisms. *Biotechnol. Res. Innov.* **2019**, *3*, 275–290. [[CrossRef](#)]
10. Raza, A.; Rehman, R.; Batool, M. Recent Review of Titania-Clay-Based Composites Emerging as Advanced Adsorbents and Photocatalysts for Degradation of Dyes over the Last Decade. *Adsorpt. Sci. Technol.* **2022**, *2022*, 3823008. [[CrossRef](#)]
11. Ellessawy, N.A.; El-Sayed, E.M.; Ali, S.; Elkady, M.F.; Elnouby, M.; Hamad, H.A. One-pot green synthesis of magnetic fullerene nanocomposite for adsorption characteristics. *J. Water Process Eng.* **2020**, *34*, 101047. [[CrossRef](#)]
12. Praveen, S.; Jegan, J.; Pushpa, T.B.; Gokulan, R.; Bulgariu, L. Biochar for removal of dyes in contaminated water: An overview. *Biochar* **2022**, *4*, 10. [[CrossRef](#)]
13. Labena, A.; Abdelhamid, A.E.; Amin, A.S.; Husien, S.; Hamid, L.; Safwat, G.; Diab, A.; Gobouri, A.A.; Azab, E. Removal of Methylene Blue and Congo Red Using Adsorptive Membrane Impregnated with Dried *Ulva fasciata* and *Sargassum dentifolium*. *Plants* **2021**, *10*, 384. [[CrossRef](#)] [[PubMed](#)]
14. Yang, G.; Wu, L.; Xian, Q.; Shen, F.; Wu, J.; Zhang, Y. Removal of Congo red and methylene blue from aqueous solutions by vermicompost-derived biochars. *PLoS ONE* **2016**, *11*, e0154562. [[CrossRef](#)] [[PubMed](#)]
15. Pai, S.; Kini, M.S.; Selvaraj, R. A review on adsorptive removal of dyes from wastewater by hydroxyapatite nanocomposites. *Environ. Sci. Pollut. Res.* **2021**, *28*, 11835–11849. [[CrossRef](#)] [[PubMed](#)]
16. Elkady, M.F.; Hassan, H.S. Invention of Hollow Zirconium Tungsto-Vanadate at Nanotube Morphological Structure for Radionuclides and Heavy Metal Pollutants Decontamination from Aqueous Solutions. *Nanoscale Res. Lett.* **2015**, *10*, 474. [[CrossRef](#)]
17. Gürses, A.; Güneş, K.; Şahin, E. Chapter 5-Removal of dyes and pigments from industrial effluents. In *Advances in Green and Sustainable Chemistry*; Sharma, S.K., Ed.; Elsevier: Amsterdam, The Netherlands, 2021; pp. 135–187. [[CrossRef](#)]
18. Mcyotto, F.; Wei, Q.; Macharia, D.K.; Huang, M.; Shen, C.; Chow, C.W.K. Effect of dye structure on color removal efficiency by coagulation. *Chem. Eng. J.* **2021**, *405*, 126674. [[CrossRef](#)]
19. Khodaie, M.; Ghasemi, N.; Moradi, B.; Rahimi, M. Removal of methylene blue from wastewater by adsorption onto Zn-activated corn husk carbon equilibrium studies. *J. Chem.* **2013**, *2013*, 383985. [[CrossRef](#)]
20. Mohammed, H.A.; Khaleefa, S.A.; Basheer, M.I. Photolysis of Methylene Blue Dye Using an Advanced Oxidation Process (Ultraviolet Light and Hydrogen Peroxide). *J. Eng. Sustain. Dev.* **2022**, *25*, 59–67. [[CrossRef](#)]
21. Beddai, A.A.; Badday, B.A.; Al-Yaqoobi, A.M.; Mejbel, M.K.; Hachim, Z.S.A.; Mohammed, M.K.A. Color Removal of Textile Wastewater Using Electrochemical Batch Recirculation Tubular Upflow Cell. *Int. J. Chem. Eng.* **2022**, *2022*, 4713399. [[CrossRef](#)]
22. Bhatia, D.; Sharma, N.R.; Singh, J.; Kanwar, R.S. Biological methods for textile dye removal from wastewater: A review. *Crit. Rev. Environ. Sci. Technol.* **2017**, *47*, 1836–1876. [[CrossRef](#)]
23. Kadhim, R.J.; Al-Ani, F.H.; Al-Shaeli, M.; Alsahy, Q.F.; Figoli, A. Removal of dyes using graphene oxide (Go) mixed matrix membranes. *Membranes* **2020**, *10*, 366. [[CrossRef](#)] [[PubMed](#)]
24. Alardhi, S.M.; Albayati, T.M.; Alrubaye, J.M. A hybrid adsorption membrane process for removal of dye from synthetic and actual wastewater. *Chem. Eng. Process Intensif.* **2020**, *157*, 108113. [[CrossRef](#)]
25. Hai, F.I.; Yamamoto, K.; Fukushima, K. Hybrid treatment systems for dye wastewater. *Crit. Rev. Environ. Sci. Technol.* **2007**, *37*, 315–377. [[CrossRef](#)]

26. Ledakowicz, S.; Pázdziar, K. Recent achievements in dyes removal focused on advanced oxidation processes integrated with biological methods. *Molecules* **2021**, *26*, 870. [[CrossRef](#)] [[PubMed](#)]
27. Wong, S.; Ghafar, N.A.; Ngadi, N.; Razmi, F.A.; Inuwa, I.M.; Mat, R.; Amin, N.A.S. Effective removal of anionic textile dyes using adsorbent synthesized from coffee waste. *Sci. Rep.* **2020**, *10*, 2928. [[CrossRef](#)]
28. Qalyoubi, L.; Al-Othman, A.; Al-Asheh, S. Recent progress and challenges of adsorptive membranes for the removal of pollutants from wastewater. Part II: Environmental applications. *Case Stud. Chem. Environ. Eng.* **2021**, *3*, 100102. [[CrossRef](#)]
29. Chen, Y.S.; Ooi, C.W.; Show, P.L.; Hoe, B.C.; Chai, W.S.; Chiu, C.-Y.; Wang, S.S.-S.; Chang, Y.-K. Removal of Ionic Dyes by Nanofiber Membrane Functionalized with Chitosan and Egg White Proteins: Membrane Preparation and Adsorption Efficiency. *Membranes* **2022**, *12*, 63. [[CrossRef](#)]
30. Tahazadeh, S.; Mohammadi, T.; Tofighy, M.A.; Khanlari, S.; Karimi, H.; Emrooz, H.B.M. Development of cellulose acetate/metal-organic framework derived porous carbon adsorptive membrane for dye removal applications. *J. Memb. Sci.* **2021**, *638*, 119692. [[CrossRef](#)]
31. Li, C.; Lou, T.; Yan, X.; Long, Y.Z.; Cui, G.; Wang, X. Fabrication of pure chitosan nanofibrous membranes as effective adsorbent for dye removal. *Int. J. Biol. Macromol.* **2018**, *106*, 768–774. [[CrossRef](#)]
32. Ma, Y.; Qi, P.; Ju, J.; Wang, Q.; Hao, L.; Wang, R.; Sui, K.; Tan, Y. Gelatin/alginate composite nanofiber membranes for effective and even adsorption of cationic dyes. *Compos. B Eng.* **2019**, *162*, 671–677. [[CrossRef](#)]
33. Cheng, J.; Zhan, C.; Wu, J.; Cui, Z.; Si, J.; Wang, Q.; Peng, X.; Turng, L.-S. Highly Efficient Removal of Methylene Blue Dye from an Aqueous Solution Using Cellulose Acetate Nanofibrous Membranes Modified by Polydopamine. *ACS Omega* **2020**, *5*, 5389–5400. [[CrossRef](#)] [[PubMed](#)]
34. Rana, J.; Goindi, G.; Kaur, N. Potential of cellulose acetate for the removal of methylene blue dye from aqueous streams. *Int. J. Innov. Technol. Explor. Eng.* **2019**, *8*, 1379–1382. [[CrossRef](#)]
35. Rambabu, K.; Velu, S. Modified cellulose acetate ultrafiltration composite membranes for enhanced dye removal. *Int. J. Chem. Sci.* **2016**, *14*, 195–205.
36. Chen, W.; Ma, H.; Xing, B. Electrospinning of multifunctional cellulose acetate membrane and its adsorption properties for ionic dyes. In *International Journal of Biological Macromolecules*; Elsevier: Amsterdam, The Netherlands, 2020; Volume 158, pp. 1342–1351. [[CrossRef](#)]
37. Abu-Dalo, M.A.; Al-Rosan, S.A.; Albiss, B.A. Photocatalytic degradation of methylene blue using polymeric membranes based on cellulose acetate impregnated with zno nanostructures. *Polymers* **2021**, *13*, 3451. [[CrossRef](#)] [[PubMed](#)]
38. Qalyoubi, L.; Al-Othman, A.; Al-Asheh, S. Recent progress and challenges on adsorptive membranes for the removal of pollutants from wastewater. Part I: Fundamentals and classification of membranes. *Case Stud. Chem. Environ. Eng.* **2021**, *3*, 100086. [[CrossRef](#)]
39. Osagie, C.; Othmani, A.; Ghosh, S.; Malloum, A.; Esfahani, Z.K.; Ahmadi, S. Dyes adsorption from aqueous media through the nanotechnology: A review. *J. Mater. Res. Technol.* **2021**, *14*, 2195–2218. [[CrossRef](#)]
40. Homaeigohar, S.; Zillohu, A.U.; Abdelaziz, R.; Hedayati, M.K.; Elbahri, M. A novel nanohybrid nanofibrous adsorbent for water purification from dye pollutants. *Materials* **2016**, *9*, 848. [[CrossRef](#)]
41. Bhatnagar, A.; Hogland, W.; Marques, M.; Sillanpää, M. An overview of the modification methods of activated carbon for its water treatment applications. *Chem. Eng. J.* **2013**, *219*, 499–511. [[CrossRef](#)]
42. Zhao, X.; Huang, C.; Zhang, S.; Wang, C. Cellulose Acetate/Activated Carbon Composite Membrane with Effective Dye Adsorption Performance. *J. Macromol. Sci. Part B Phys.* **2019**, *58*, 909–920. [[CrossRef](#)]
43. Moosavi, S.; Lai, C.W.; Gan, S.; Zamiri, G.; Pivehzhani, O.A.; Johan, M.R. Application of efficient magnetic particles and activated carbon for dye removal from wastewater. *ACS Omega* **2020**, *5*, 20684–20697. [[CrossRef](#)]
44. Shokry, H.; Elkady, M.; Hamad, H. Nano activated carbon from industrial mine coal as adsorbents for removal of dye from simulated textile wastewater: Operational parameters and mechanism study. *J. Mater. Res. Technol.* **2019**, *8*, 4477–4488. [[CrossRef](#)]
45. Kanawade, S.M.; Gaikwad, R.W. Removal of Methylene Blue from Effluent by Using Activated Carbon and Water Hyacinth as Adsorbent. *Int. J. Chem. Eng. Appl.* **2011**, *2*, 317–319. [[CrossRef](#)]
46. Köseoğlu, E.; Akmil-Başar, C. Preparation, structural evaluation and adsorptive properties of activated carbon from agricultural waste biomass. *Adv. Powder Technol.* **2015**, *26*, 811–818. [[CrossRef](#)]
47. Malik, A. Environmental challenge vis a vis opportunity: The case of water hyacinth. *Environ. Int.* **2007**, *33*, 122–138. [[CrossRef](#)] [[PubMed](#)]
48. Mahamadi, C. Water hyacinth as a biosorbent: A review. *Afr. J. Environ. Sci. Tech.* **2012**, *5*, 1137–1145. [[CrossRef](#)]
49. Li, F.; He, X.; Srishti, A.; Song, S.; Tan, H.T.W.; Sweeney, D.J.; Ghosh, S.; Wang, C.-H. Water hyacinth for energy and environmental applications: A review. *Bioresour. Technol.* **2021**, *327*, 124809. [[CrossRef](#)] [[PubMed](#)]
50. Shokry, H.; Elkady, M.; Salama, E. Eco-friendly magnetic activated carbon nano-hybrid for facile oil spills separation. *Sci. Rep.* **2020**, *10*, 10265. [[CrossRef](#)] [[PubMed](#)]
51. Strathmann, H.; Scheible, P.; Baker, R.W. A rationale for the preparation of Loeb-Sourirajan-type cellulose acetate membranes. *J. Appl. Polym. Sci.* **1971**, *15*, 811–828. [[CrossRef](#)]
52. Sahraei, R.; Shahalizade, T.; Ghaemy, M.; Mahdavi, H. Fabrication of cellulose acetate/Fe<sub>3</sub>O<sub>4</sub>@GO-APTS-poly(AMPS-co-MA) mixed matrix membrane and its evaluation on anionic dyes removal. *Cellulose* **2018**, *25*, 3519–3532. [[CrossRef](#)]

53. Ghaseminezhad, S.M.; Barikani, M.; Salehirad, M. Development of graphene oxide-cellulose acetate nanocomposite reverse osmosis membrane for seawater desalination. *Compos. B Eng.* **2019**, *161*, 320–327. [[CrossRef](#)]
54. Thamer, B.M.; Aldalbahi, A.; Moydeen, M.A.; Rahaman, M.; El-Newehy, M.H. Modified electrospun polymeric nanofibers and their nanocomposites as nanoadsorbents for toxic dye removal from contaminated waters: A review. *Polymers* **2021**, *23*, 20. [[CrossRef](#)] [[PubMed](#)]
55. Subrahmanya, T.M.; Arshad, A.B.; Lin, P.T.; Widakdo, J.; Makari, H.K.; Austria, H.F.; Hu, C.C.; Lai, J.Y.; Hung, W.S. A review of recent progress in polymeric electrospun nanofiber membranes in addressing safe water global issues. *RSC Adv.* **2021**, *11*, 9638–9663. [[CrossRef](#)]
56. Elkady, M.; Shokry, H.; Hamad, H. New activated carbon from mine coal for adsorption of dye in simulated water or multiple heavy metals in real wastewater. *Materials* **2020**, *13*, 2498. [[CrossRef](#)] [[PubMed](#)]
57. Liu, Y.; Liu, X.; Dong, W.; Zhang, L.; Kong, Q.; Wang, W. Efficient Adsorption of Sulfamethazine onto Modified Activated Carbon: A Plausible Adsorption Mechanism. *Sci. Rep.* **2017**, *7*, 12437. [[CrossRef](#)] [[PubMed](#)]
58. Yu, X.; Han, Z.; Fang, S.; Chang, C.; Han, X. Optimized Preparation of High Value-Added Activated Carbon and Its Adsorption Properties for Methylene Blue. *Int. J. Chem. React. Eng.* **2019**, *17*, 20180267. [[CrossRef](#)]
59. Kebir, M.; Trari, M.; Maachi, R.; Nasrallah, N.; Amrane, A. Valorization of Inula viscosa waste extraction, modeling of isotherm, and kinetic for the tartrazine dye adsorption. *Desalination Water Treat* **2015**, *54*, 2806–2816. [[CrossRef](#)]
60. Kalyani, P.; Anitha, A. Refuse derived energy-tea derived boric acid activated carbon as an electrode material for electrochemical capacitors. *Port. Electrochim. Acta* **2013**, *31*, 165–174. [[CrossRef](#)]
61. Ding, B.; Li, C.; Hotta, Y.; Kim, J.; Kuwaki, O.; Shiratori, S. Conversion of an electrospun nanofibrous cellulose acetate mat from a super-hydrophilic to super-hydrophobic surface. *Nanotechnology* **2006**, *17*, 4332–4339. [[CrossRef](#)]
62. Namjoufar, M.; Farzi, A.; Karimi, A. Removal of Acid Brown 354 from wastewater by aminized cellulose acetate nanofibers: Experimental and theoretical study of the effect of different parameters on adsorption efficiency. *Water Sci. Technol.* **2021**, *83*, 1649–1661. [[CrossRef](#)]
63. Sudiarti, T.; Wahyuningrum, D.; Bundjali, B.; Arcana, I.M. Mechanical strength and ionic conductivity of polymer electrolyte membranes prepared from cellulose acetate-lithium perchlorate. *IOP Conf. Ser. Mater. Sci. Eng.* **2017**, *223*, 012052. [[CrossRef](#)]
64. Baniasadi, J.; Shabani, Z.; Mohammadi, T.; Sahebi, S. Enhanced performance and fouling resistance of cellulose acetate forward osmosis membrane with the spatial distribution of TiO<sub>2</sub> and Al<sub>2</sub>O<sub>3</sub> nanoparticles. *J. Chem. Technol. Biotechnol.* **2021**, *96*, 147–162. [[CrossRef](#)]
65. Silva, M.A.; Hilliou, L.; de Amorim, M.T.P. Fabrication of pristine-multiwalled carbon nanotubes/cellulose acetate composites for removal of methylene blue. *Polym. Bull.* **2020**, *77*, 623–653. [[CrossRef](#)]
66. Aboamera, N.M.; Mohamed, A.; Salama, A.; Osman, T.A.; Khattab, A. An effective removal of organic dyes using surface functionalized cellulose acetate/graphene oxide composite nanofibers. *Cellulose* **2018**, *25*, 4155–4166. [[CrossRef](#)]